










TECH BRIEFS

NATIONAL AERONAUTICS AND SPACE ADMINISTRATION

-  **Technology Focus**
-  **Computers/Electronics**
-  **Software**
-  **Materials**
-  **Mechanics**
-  **Machinery/Automation**
-  **Manufacturing**
-  **Bio-Medical**
-  **Physical Sciences**
-  **Information Sciences**
-  **Books and Reports**

INTRODUCTION

Tech Briefs are short announcements of innovations originating from research and development activities of the National Aeronautics and Space Administration. They emphasize information considered likely to be transferable across industrial, regional, or disciplinary lines and are issued to encourage commercial application.

Availability of NASA Tech Briefs and TSPs

Requests for individual Tech Briefs or for Technical Support Packages (TSPs) announced herein should be addressed to

National Technology Transfer Center

Telephone No. (800) 678-6882 or via World Wide Web at www2.nttc.edu/leads/

Please reference the control numbers appearing at the end of each Tech Brief. Information on NASA's Innovative Partnerships Program (IPP), its documents, and services is also available at the same facility or on the World Wide Web at <http://ipp.nasa.gov>.

Innovative Partnerships Offices are located at NASA field centers to provide technology-transfer access to industrial users. Inquiries can be made by contacting NASA field centers and Mission Directorates listed below.

NASA Field Centers and Program Offices

Ames Research Center

Lisa L. Lockyer
(650) 604-1754
lisa.l.lockyer@nasa.gov

Dryden Flight Research Center

Gregory Poteat
(661) 276-3872
greg.poteat@dfrc.nasa.gov

Goddard Space Flight Center

Nona Cheeks
(301) 286-5810
Nona.K.Cheeks.1@nasa.gov

Jet Propulsion Laboratory

Ken Wolfenbarger
(818) 354-3821
james.k.wolfenbarger@jpl.nasa.gov

Johnson Space Center

Helen Lane
(713) 483-7165
helen.w.lane@nasa.gov

Kennedy Space Center

Jim Aliberti
(321) 867-6224
Jim.Aliberti-1@nasa.gov

Langley Research Center

Ray P. Turcotte
(757) 864-8881
r.p.turcotte@larc.nasa.gov

John H. Glenn Research Center at Lewis Field

Robert Lawrence
(216) 433-2921
robert.f.lawrence@nasa.gov

Marshall Space Flight Center

Vernotto McMillan
(256) 544-2615
vernotto.mcmillan@msfc.nasa.gov

Stennis Space Center

John Bailey
(228) 688-1660
john.w.bailey@nasa.gov

NASA Mission Directorates

At NASA Headquarters there are four Mission Directorates under which there are seven major program offices that develop and oversee technology projects of potential interest to industry:

Carl Ray

Small Business Innovation Research Program (SBIR) & Small Business Technology Transfer Program (STTR)
(202) 358-4652
carl.g.ray@nasa.gov

Frank Schowengerdt

Innovative Partnerships Program (Code TD)
(202) 358-2560
fschowen@hq.nasa.gov

John Mankins

Exploration Systems Research and Technology Division
(202) 358-4659
john.c.mankins@nasa.gov

Terry Hertz

Aeronautics and Space Mission Directorate
(202) 358-4636
thertz@mail.hq.nasa.gov

Glen Mucklow

Mission and Systems Management Division (SMD)
(202) 358-2235
gmucklow@mail.hq.nasa.gov

Granville Paules

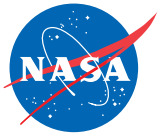
Mission and Systems Management Division (SMD)
(202) 358-0706
gpaules@mtpe.hq.nasa.gov

Gene Trinh

Human Systems Research and Technology Division (ESMD)
(202) 358-1490
eugene.h.trinh@nasa.gov

John Rush

Space Communications Office (SOMD)
(202) 358-4819
john.j.rush@nasa.gov



TECH BRIEFS

NATIONAL AERONAUTICS AND SPACE ADMINISTRATION



5 Technology Focus: Test & Measurement

- 5 Nearly Direct Measurement of Relative Permittivity
- 6 DCS-Neural-Network Program for Aircraft Control and Testing
- 6 Dielectric Heaters for Testing Spacecraft Nuclear Reactors
- 6 Using Doppler Shifts of GPS Signals To Measure Angular Speed
- 7 Monitoring Temperatures of Tires Using Luminescent Materials



9 Electronics/Computers

- 9 Highly Efficient Multilayer Thermoelectric Devices
- 9 Very High-Speed Digital Video Capability for In-Flight Use
- 10 MMIC DHBT Common-Base Amplifier for 172 GHz
- 11 Modular, Microprocessor-Controlled Flash Lighting System



13 Software

- 13 Generic Environment for Simulating Launch Operations
- 13 Modular Aero-Propulsion System Simulation
- 13 X-Windows Socket Widget Class
- 13 Infrastructure for Rapid Development of Java GUI Programs
- 14 Processing Raman Spectra of High-Pressure Hydrogen Flames
- 14 X-Windows Information Sharing Protocol Widget Class
- 14 Simulating Humans as Integral Parts of Spacecraft Missions
- 14 Analyzing Power Supply and Demand on the ISS



15 Materials

- 15 Polyimides From a-BPDA and Aromatic Diamines
- 16 Making Plant-Support Structures From Waste Plant Fiber



17 Mechanics

- 17 Large Deployable Reflectarray Antenna
- 17 Periodically Discharging, Gas-Coalescing Filter



19 Manufacturing & Prototyping

- 19 Ion Milling On Steps for Fabrication of Nanowires



21 Bio-Medical

- 21 Neuro-Prosthetic Implants With Adjustable Electrode Arrays
- 22 Microfluidic Devices for Studying Biomolecular Interactions
- 23 Studying Functions of All Yeast Genes Simultaneously



25 Physical Sciences

- 25 Polarization Phase-Compensating Coats for Metallic Mirrors
- 25 Tunable-Bandwidth Filter System



27 Books & Reports

- 27 Methodology for Designing Fault-Protection Software
- 27 Ground-Based Localization of Mars Rovers

This document was prepared under the sponsorship of the National Aeronautics and Space Administration. Neither the United States Government nor any person acting on behalf of the United States Government assumes any liability resulting from the use of the information contained in this document, or warrants that such use will be free from privately owned rights.



Nearly Direct Measurement of Relative Permittivity

The only quantities measured are two voltages.

John F. Kennedy Space Center, Florida

A recently conceived technique for determining the relative permittivity of a material sample at a given frequency is more nearly direct than are prior techniques that involve measurement of such related non-electrical quantities as the size, shape, and/or weight of the specimen. The present technique involves only measurement of two voltages at the frequency in question, followed by calculation of the ratio between the voltages.

The technique requires two circuits — a test circuit and a reference circuit — that are identical except as described below. Each circuit includes a capacitor C_1 connected in series with a much larger capacitor C_2 to form a voltage divider (see figure). C_1 is a parallel-plate capacitor.

The top electrode of C_1 is connected to an AC signal source of voltage V_a at the frequency of interest. The top electrode of C_1 is surrounded by a guard electrode that, in turn, is surrounded by a grounded electrode. The bottom electrode of C_1 is connected to the top electrode of C_2 . The bottom electrode of C_2 is grounded.

The volume enclosed by the top, bottom, and guard electrodes of C_1 constitutes a sample cell. A material sample, having relative permittivity k at the frequency of interest, is placed in the sample cell. The exact shape and size of the sample volume is not critical and can be chosen to fit the material sample. What is critical is that (a) C_2 in both circuits be identical and (b) the sample cell in the test circuit have the same size and shape

as that in the reference circuit, so that the capacitances of the two sample cells are proportional to the permittivities of their contents. Then the capacitances of the two sample cells are given by

$$C_{1\text{test}} = k_{\text{test}} C_0 \text{ and } C_{1\text{reference}} = k_{\text{reference}} C_0,$$

where C_0 = the capacitance of either sample cell when it is empty.

For each circuit, the voltage between the (C_1, C_2) junction and ground is given by

$$V_2 = V_a C_1 / (C_1 + C_2).$$

Inasmuch as $C_2 \gg C_1$, this voltage is closely approximated by

$$V_2 \approx V_a C_1 / C_2.$$

For the test and reference assemblies, respectively, this relation becomes

$$V_{2\text{test}} \approx V_a C_{1\text{test}} / C_2 = V_a k_{\text{test}} C_0 / C_2 \text{ and } V_{2\text{reference}} \approx V_a C_{1\text{reference}} / C_2 = V_a k_{\text{reference}} C_0 / C_2.$$

Then taking the ratio between the two V_2 measurements, one obtains

$$k_{\text{test}} / k_{\text{reference}} \approx V_{2\text{test}} / V_{2\text{reference}}.$$

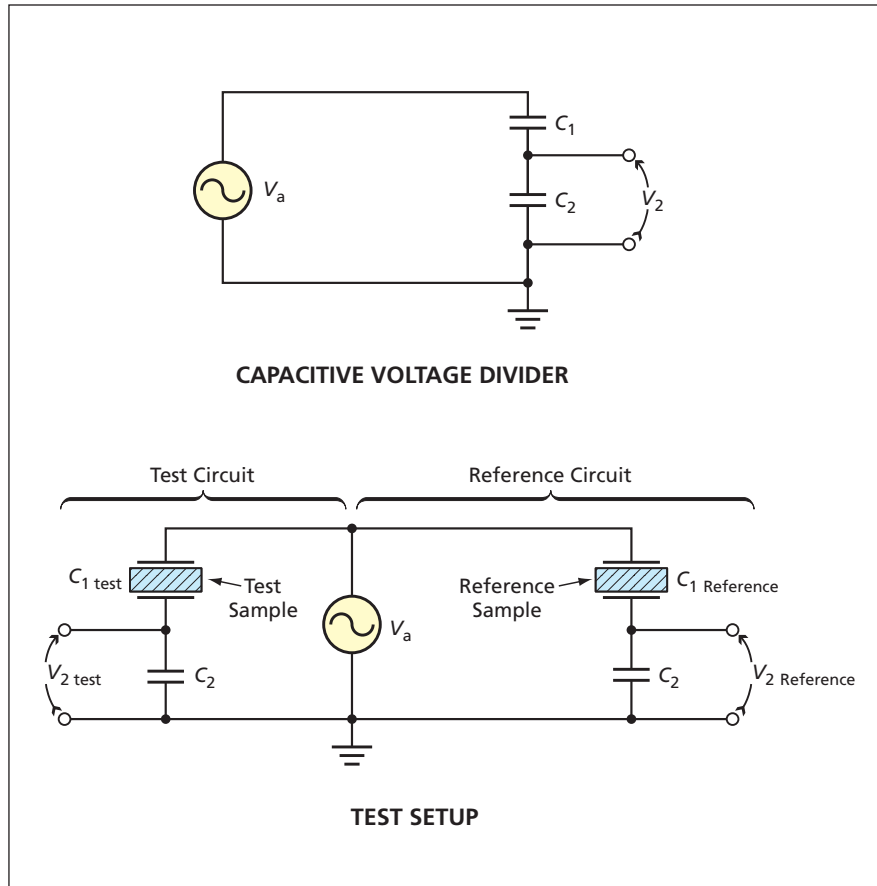
The sample can be a liquid, a solid, a granular material, or a mixture of materials: the technique is valid for almost any dielectric material or combination of materials, the only requirement being that the sample fill the sample cell in the test circuit. If the sample cell in the reference circuit is kept empty (in which case $k_{\text{reference}} = 1$), then the relative permittivity of the material sample in the test cell is given simply by

$$k_{\text{test}} \approx V_{2\text{test}} / V_{2\text{reference}}.$$

In the original application for which the technique was developed, the material to be tested was to be a granular one containing an unknown amount of moisture (representing moist soil), while the reference material was to be a dry sample of the same granular material. Assuming that the permittivity varies linearly with the moisture constant, one could estimate the moisture content as being approximately proportional to

$$(k_{\text{test}} / k_{\text{reference}}) - 1 \approx (V_{2\text{test}} / V_{2\text{reference}}) - 1.$$

This work was done by Carlos I. Calle of Kennedy Space Center and James G. Mantovani, independent contractor. For further information, contact Carlos I. Calle at (321) 867-3274. KSC-12572



The Ratio Between the Permittivities of the test and reference samples is closely approximated by $V_{2\text{test}}/V_{2\text{reference}}$, as long as the requirements stated in the text are satisfied. For the sake of simplicity, the guard electrodes and associated amplifier circuitry are omitted from the diagrams.

DCS-Neural-Network Program for Aircraft Control and Testing

Ames Research Center, Moffett Field, California

A computer program implements a dynamic-cell-structure (DCS) artificial neural network that can perform such tasks as learning selected aerodynamic characteristics of an airplane from wind-tunnel test data and computing real-time stability and control derivatives of the airplane for use in feedback linearized control. A DCS neural network is one of several types of neural networks that can incorporate additional nodes in order to rapidly learn increasingly complex relationships between inputs and outputs. In the DCS neural network implemented by the

present program, the insertion of nodes is based on accumulated error. A competitive Hebbian learning rule (a supervised-learning rule in which connection weights are adjusted to minimize differences between actual and desired outputs for training examples) is used. A Kohonen-style learning rule (derived from a relatively simple training algorithm, implements a Delaunay triangulation layout of neurons) is used to adjust node positions during training. Neighborhood topology determines which nodes are used to estimate new values. The network learns, start-

ing with two nodes, and adds new nodes sequentially in locations chosen to maximize reductions in global error. At any given time during learning, the error becomes homogeneously distributed over all nodes.

This program was written by Charles C. Jorgensen of Ames Research Center. Further information is contained in a TSP (see page 1).

Inquiries concerning rights for the commercial use of this invention should be addressed to the Technology Partnerships Division, Ames Research Center, (650) 604-2954. Refer to ARC-14555-1.

Dielectric Heaters for Testing Spacecraft Nuclear Reactors

Marshall Space Flight Center, Alabama

A document proposes the development of radio-frequency- (RF)-driven dielectric heaters for non-nuclear thermal testing of the cores of nuclear-fission reactors for spacecraft. Like the electrical-resistance heaters used heretofore for such testing, the dielectric heaters would be inserted in the reactors in place of nuclear fuel rods. A typical heater according to the proposal would consist of a rod of lossy dielectric material sized and shaped like a fuel rod and containing an electrically conductive rod along its center line. Exploiting the dielectric loss mechanism that is usually

considered a nuisance in other applications, an RF signal, typically at a frequency ≤ 50 MHz and an amplitude between 2 and 5 kV, would be applied to the central conductor to heat the dielectric material. The main advantage of the proposal is that the wiring needed for the RF dielectric heating would be simpler and easier to fabricate than is the wiring needed for resistance heating. In some applications, it might be possible to eliminate all heater wiring and, instead, beam the RF heating power into the dielectric rods from external antennas.

This work was done by William Herbert Sims of Marshall Space Flight Center, Leo Bitteker of the University of California, and Thomas Godfroy of the University of Michigan. Further information is contained in a TSP (see page 1).

This invention is owned by NASA, and a patent application has been filed. For further information, contact Sammy Nabors, MSFC Commercialization Assistance Lead, at sammy.a.nabors@nasa.gov. Refer to MFS-31823-1.

Using Doppler Shifts of GPS Signals To Measure Angular Speed Gyroscopes could be eliminated, reducing costs.

Goddard Space Flight Center, Greenbelt, Maryland

A method has been proposed for extracting information on the rate of rotation of an aircraft, spacecraft, or other body from differential Doppler shifts of Global Positioning System (GPS) signals received by antennas mounted on the body. In principle, the method should be capable of yielding low-noise estimates of rates of rotation. The method could eliminate the need for gyroscopes to measure rates of rotation.

The method is based on the fact that for a given signal of frequency f_i transmitted by a given GPS satellite, the dif-

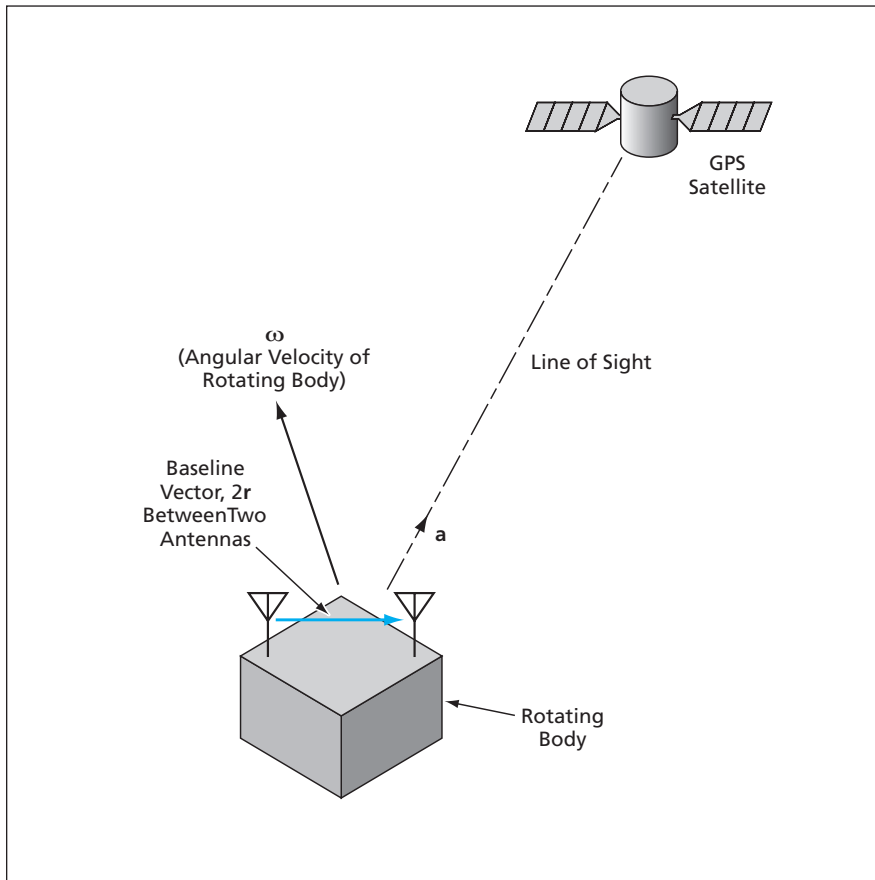
ferential Doppler shift is attributable to the difference between those components of the instantaneous translational velocities of the antennas that lie along the line of sight from the antennas to the GPS satellite. On the basis of straightforward geometric considerations (see figure), it can be readily shown that the differential Doppler shift is related to the angular velocity (ω) of the rotating body by

$$f_{r1} - f_{r2} = 2f_i(\omega \times \mathbf{r}) \cdot \mathbf{a} / c,$$

where f_{r1} and f_{r2} are the instantaneous Doppler-shifted frequencies of the replicas of the f_i signal received by the two an-

tennas, \mathbf{r} is half of the baseline vector between the two antennas, \mathbf{a} is a unit vector along the line of sight from the antennas to the GPS satellite, and c is the speed of light.

It must be noted that the equation above can be solved to obtain only partial information about ω . However, if there are three or more antennas and if signals can be received from two or more GPS satellites, then one can form simultaneous independent equations for different pairs of antennas and different unit vectors that can be solved to obtain all of the components of ω .



Two Antennas on a Rotating Body would have different components of velocity along the line of sight to a GPS satellite, giving rise to different Doppler shifts of the two received GPS signals.

It is assumed that the received f_{r1} and f_{r2} signals would be subjected to the usual GPS processing, including phase-shifting and cross-correlation with the applicable GPS pseudorandom-noise code for acquisition and tracking. To obtain the differential Doppler frequency $f_{r1} - f_{r2}$ for a given antenna pair and a given GPS satellite, the f_{r1} and f_{r2} signals would be fed to a multiplier. By virtue of the trigonometric identity for the product of sines of different arguments, the low-frequency multiplier output would be a sinusoidal waveform of frequency $f_{r1} - f_{r2}$. For high accuracy, the multiplier output could be fed to a subsystem containing a zero-crossing detector coupled with a counter driven by a quartz-crystal clock circuit. Such a subsystem could accumulate counts over times long enough to enable estimation of periods of rotation to within microseconds.

This work was done by Charles E. Campbell, Jr., of Goddard Space Flight Center. Further information is contained in a TSP (see page 1).

This invention has been patented by NASA (U.S. Patent No. 6,593,879). Inquiries concerning nonexclusive or exclusive license for its commercial development should be addressed to the Patent Counsel, Goddard Space Flight Center, (301) 286-7351. Refer to GSC-14087-1.

Monitoring Temperatures of Tires Using Luminescent Materials

Hot spots are detected and monitored as indications of local damage.

John H. Glenn Research Center, Cleveland, Ohio

A method of noncontact, optical monitoring of the surface temperature of a tire has been devised to enable the use of local temperature rise as an indication of potential or impending failures. The method involves the use of temperature-sensitive paint (or filler): Temperature-sensitive luminescent dye molecules or other luminescent particles are incorporated into a thin, flexible material coating the tire surface of interest. (Alternatively, in principle, the luminescent material could be incorporated directly into the tire rubber, though this approach has not yet been tested.) The coated surface is illuminated with shorter-wavelength light to excite longer-wavelength luminescence, which is

observed by use of a charge-coupled-device camera or a photodetector (see Figure 1).

If temporally constant illumination is used, then the temperature can be deduced from the known temperature dependence of the intensity response of the luminescence. If pulsed illumination is used, then the temperature can be deduced from the known temperature dependence of the time or frequency response of the luminescence. If sinusoidally varying illumination is used, then the temperature can be deduced from the known temperature dependence of the phase response of the luminescence.

Unlike a prior method of monitoring the temperature at a fixed spot on a

tire by use of a thermocouple, this method is not restricted to one spot and can, therefore, yield information on the spatial distribution of temperature: in particular, it enables the discovery of newly forming hot spots where damage may be starting. Also unlike in the thermocouple method, the measurements in this method are not vulnerable to breakage of wires in repeated flexing of the tire. Moreover, unlike in another method in which infrared radiation is monitored as an indication of surface temperature, the luminescence measurements in this method are not significantly affected by changes in infrared emissivity.

This method has been demonstrated in application to the outside surface of

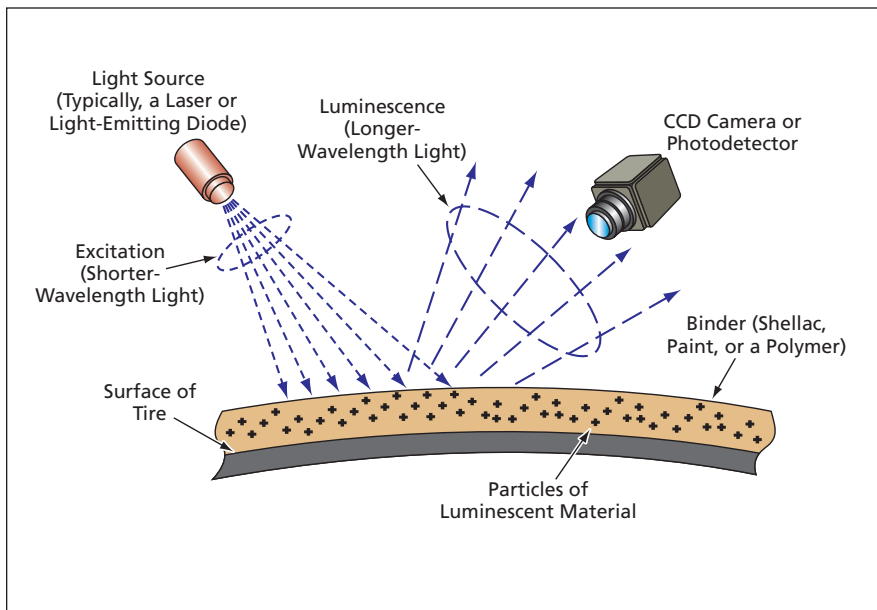


Figure 1. Luminescent Dye Molecules or Other Particles in a flexible binder on the surface of a tire are illuminated. The longer-wavelength luminescence is observed as an indication of temperature.

a tire (see Figure 2), using both constant and pulsed light sources for illumination and cooled, slow-scan, gated CCD cameras for detection. For observing the temperature of the inside surface of a tire (this has not yet been done), it would probably be necessary

to use fiber optics and/or windows for coupling excitation light into, and coupling luminescence out of, the interior volume.

This work was done by Timothy J. Bencic of Glenn Research Center. Further information is contained in a TSP (see page 1).

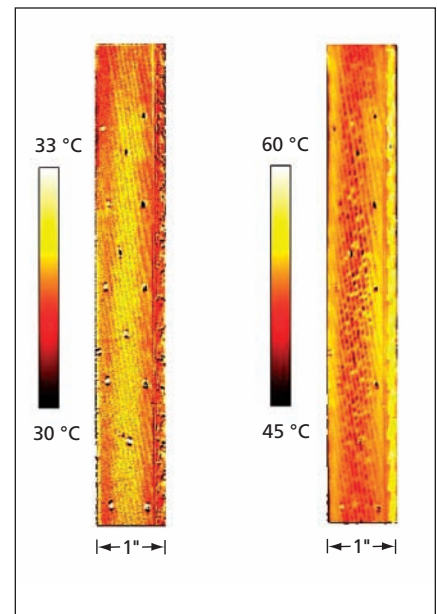


Figure 2. An *In-Situ* Thermal Map shows a tire sample during cyclic tensile-tensile loading. The temperature increases with increased loading.

Inquiries concerning rights for the commercial use of this invention should be addressed to NASA Glenn Research Center, Innovative Partnerships Office, Attn: Steve Fedor, Mail Stop 4-8, 21000 Brookpark Road, Cleveland, Ohio 44135. Refer to LEW-17417-1.



Highly Efficient Multilayer Thermoelectric Devices

Temperature differences as great as 50 K can be produced at or near room temperature.

Goddard Space Flight Center, Greenbelt, Maryland

Multilayer thermoelectric devices now at the prototype stage of development exhibit a combination of desirable characteristics, including high figures of merit and high performance/cost ratios. These devices are capable of producing temperature differences of the order of 50 K in operation at or near room temperature. A solvent-free batch process for mass production of these state-of-the-art thermoelectric devices has also been developed.

Like prior thermoelectric devices, the present ones have commercial potential mainly by virtue of their utility as means of controlled cooling (and/or, in some cases, heating) of sensors, integrated circuits, and temperature-critical components of scientific instruments. The advantages of thermoelectric devices for such uses include no

need for circulating working fluids through or within the devices, generation of little if any noise, and high reliability. The disadvantages of prior thermoelectric devices include high power consumption and relatively low coefficients of performance.

The present development program was undertaken in the hope of reducing the magnitudes of the aforementioned disadvantages and, especially, obtaining higher figures of merit for operation at and near room temperature. Accomplishments of the program thus far include development of an algorithm to estimate the heat extracted by, and the maximum temperature drop produced by, a thermoelectric device; solution of the problem of exchange of heat between a thermoelectric cooler and a water-cooled copper block; retrofitting of a

vacuum chamber for depositing materials by sputtering; design of masks; and fabrication of multilayer thermoelectric devices of two different designs, denoted I and II.

For both the I and II designs, the thicknesses of layers are of the order of nanometers. In devices of design I, non-consecutive semiconductor layers are electrically connected in series. Devices of design II contain superlattices comprising alternating electron-acceptor (p)-doped and electron-donor (n)-doped, nanometer-thick semiconductor layers.

This work was done by Ali Boufelfel of Sigma Technologies International, Inc. for Goddard Space Flight Center. For further information, contact the Goddard Innovative Partnerships Office at (301) 286-5810. GSC-14786-1

Very High-Speed Digital Video Capability for In-Flight Use

Flight-qualified video system provides very-high-speed color digital-video imaging up to 10,000 pictures per second at flight speeds up to Mach 2.

Dryden Flight Research Center, Edwards, California

A digital video camera system has been qualified for use in flight on the NASA supersonic F-15B Research Testbed aircraft. This system is capable of very-high-speed color digital imaging at flight speeds up to Mach 2. The components of this system have been ruggedized and shock-mounted in the aircraft to survive the severe pressure, temperature, and vibration of the flight environment. The system includes two synchronized camera subsystems installed in fuselage-mounted camera pods (see Figure 1).

Each camera subsystem comprises a camera controller/recorder unit and a camera head. The two camera subsystems are synchronized by use of an M-Hub™ synchronization unit. Each camera subsystem is capable of recording at a rate up to 10,000 pictures per second (pps). A state-of-the-art complementary metal oxide/semiconductor (CMOS)

sensor in the camera head has a maximum resolution of 1,280×1,024 pixels at 1,000 pps. Exposure times of the electronic shutter of the camera range from

1/200,000 of a second to full open. The recorded images are captured in a dynamic random-access memory (DRAM) and can be downloaded directly to a per-



Figure 1. Two Very-High-Speed Digital Video Cameras are mounted in forward and aft camera pods, respectively, on the F-15B Research Testbed aircraft. The cameras are positioned to obtain photogrammetric data of simulated space-shuttle external-tank thermal-insulation foam debris released from a fixture under the centerline of the aircraft at flight speed up to Mach 2.

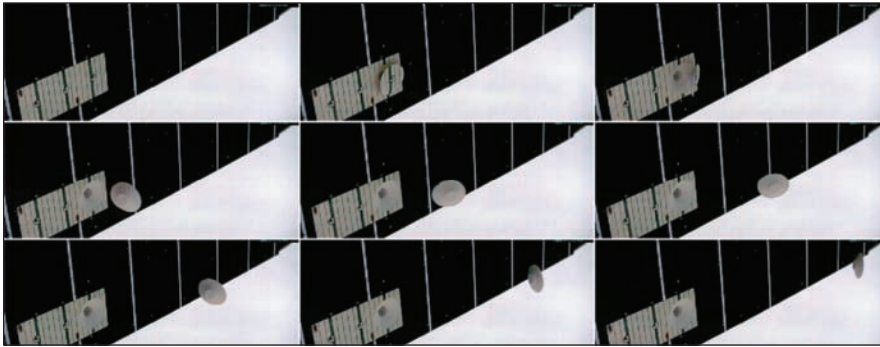


Figure 2. **Frame Captures of High-Speed Digital Video** are showing ejection of "divot" debris from F-15B Aerodynamic Flight Test Fixture underneath the aircraft centerline. Flight conditions for the divot ejection are Mach 2 at 48,250 ft (14.7 km) altitude. Video frame rate is 2,000 pictures per second, exposure rate is 50 microseconds, and resolution is 1280x512 pixels. (Sequence starts at upper left frame and proceeds from left to right.)

sonal computer or saved on a compact flash memory card. In addition to the high-rate recording of images, the system can display images in real time at 30 pps. Inter Range Instrumentation Group (IRIG) time code can be inserted into

the individual camera controllers or into the M-Hub unit. The video data could also be used to obtain quantitative, three-dimensional trajectory information.

The first use of this system was in support of the Space Shuttle Return to

Flight effort. Data were needed to help in understanding how thermally insulating foam is shed from a space-shuttle external fuel tank during launch. The cameras captured images of simulated external tank debris ejected from a fixture mounted under the centerline of the F-15B aircraft. Digital video was obtained at subsonic and supersonic flight conditions, including speeds up to Mach 2 and altitudes up to 50,000 ft (15.24 km). The digital video was used to determine the structural survivability of the debris in a real flight environment and quantify the aerodynamic trajectories of the debris.

This work was done by Stephen Corda, Ting Tseng, Matthew Reaves, Kendall Mauldin, and Donald Whiteman of Dryden Flight Research Center. Further information is contained in a TSP (see page 1). DRC-05-16

MMIC DHBT Common-Base Amplifier for 172 GHz

This single-transistor circuit performs comparably to a prior four-transistor circuit.

NASA's Jet Propulsion Laboratory, Pasadena, California

Figure 1 shows a single-stage monolithic microwave integrated circuit (MMIC) power amplifier in which the gain element is a double-heterojunction bipolar transistor (DHBT) connected in common-base configuration. This amplifier, which has been demonstrated to function well at a frequency of 172 GHz, is part of a continuing effort to develop compact, efficient amplifiers for scientific instrumentation, wide-band communication systems, and radar systems that will operate at frequencies up to and beyond 180 GHz.

The transistor is fabricated from a layered structure formed by molecular-beam epitaxy in the InP/InGaAs material system. A highly doped InGaAs base layer and a collector layer are fabricated from the layered structure in a triple mesa process. The transistor includes two separate emitter fingers, each having dimensions of 0.8 by 12 μm . The common-base configuration was chosen for its high maximum stable gain in the frequency band of interest. The input-matching network is designed for high bandwidth. The output of the transistor is matched to a load line for maximum saturated output power under large-signal conditions, rather than being matched for maximum gain under small-signal conditions.

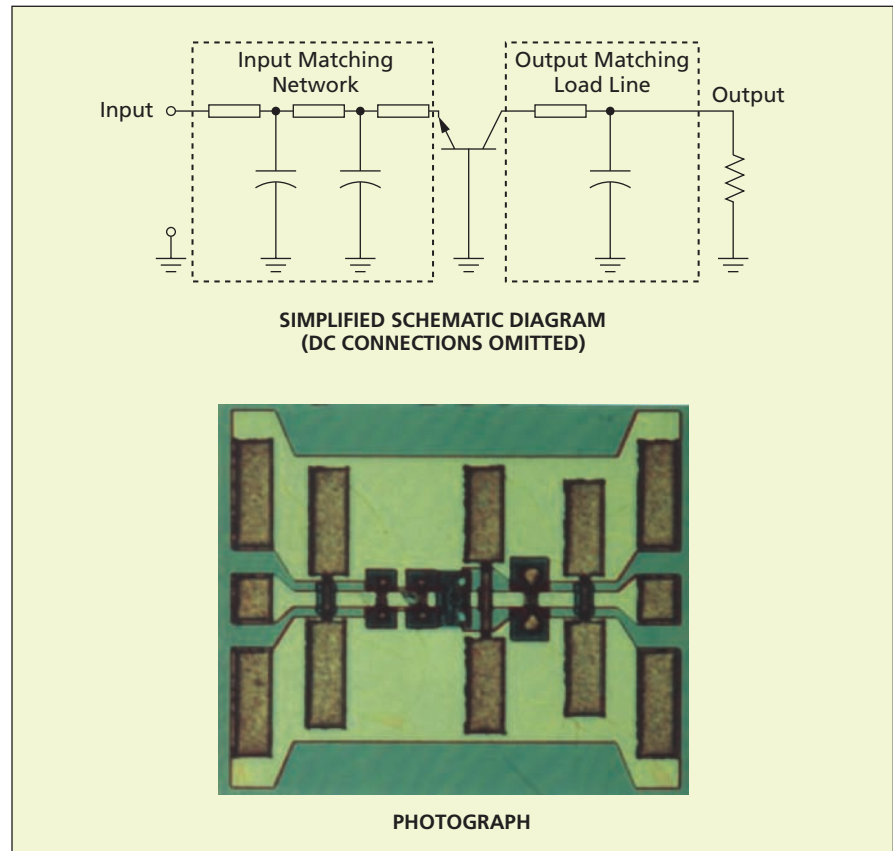


Figure 1. This **Common-Base, Single-Transistor Amplifier** is designed to provide useful power gain in the frequency band of 170 to 180 GHz.

In a test at a frequency of 172 GHz, the amplifier was found to generate an output power of 7.5 mW, with approximately 5 dB of large-signal gain (see Figure 2). Moreover, the amplifier exhibited a peak small-signal gain of 7 dB at a frequency of 176 GHz. This performance of this MMIC single-stage amplifier containing only a single transistor represents a significant advance in the state of the art, in that it rivals the 170-GHz performance of a prior MMIC three-stage, four-transistor amplifier. [The prior amplifier was reported in "MMIC HEMT Power Amplifier for 140 to 170 GHz" (NPO-30127), *NASA Tech Briefs*, Vol. 27, No. 11 (November 2003), page 49.]

This amplifier is the first heterojunction-bipolar-transistor (HBT) amplifier built for medium power operation in this frequency band. The performance of the amplifier as measured in the aforementioned tests suggests that InP/InGaAs HBTs may be superior to high-electron-mobility (HEMT) transistors in that the HBTs may offer more gain per stage and more output power per transistor.

This work was done by Vamsi Paidi, Zack Griffith, Yun Wei, Mattias Dahlstrom, Miguel Urteaga, and Mark Rodwell of the University of California at Santa Barbara and Lorene Samoska, King Man Fung, and Erich Schlecht of Caltech for NASA's Jet

Propulsion Laboratory. Further information is contained in a TSP (see page 1).

In accordance with Public Law 96-517, the contractor has elected to retain title to this invention. Inquiries concerning rights for its commercial use should be addressed to:

*Innovative Technology Assets Management
JPL*

*Mail Stop 202-233
4800 Oak Grove Drive
Pasadena, CA 91109-8099
(818) 354-2240*

*E-mail: iaoffice@jpl.nasa.gov
Refer to NPO-40956, volume and number of this NASA Tech Briefs issue, and the page number.*

Modular, Microprocessor-Controlled Flash Lighting System

This system can be readily reconfigured to satisfy different requirements.

John H. Glenn Research Center, Cleveland, Ohio

A microprocessor-controlled lighting system generates brief, precisely timed, high-intensity flashes of light for scientific imaging at frame rates up to about 1 kHz. The system includes an array of light-emitting diodes (LEDs) that are driven in synchronism with an externally generated timing signal (for example, a timing signal generated by a video camera). The light output can be varied in peak intensity, pulse duration, pulse delay, and pulse rate, all depending on the timing signal and associated externally generated control signals.

The array of LEDs comprises as many as 16 LED panels that can be attached together. Each LED panel is a module consisting of a rectangular subarray of 10 by 20 LEDs of advanced design on a printed-circuit board in a mounting frame with a power/control connector. The LED panels are controlled by an LED control module that contains an AC-to-DC power supply, a control

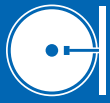
board, and 8 LED-panel driver boards. In prior LED panels, the LEDs are packaged at less than maximum areal densities in bulky metal housings that reduce effective active areas. In contrast, in the present LED panels, the LEDs are packed at maximum areal density so as to afford 100-percent active area and so that when panels are joined side by side to form the array, there are no visible seams between them and the proportion of active area is still 100 percent. Each panel produces an illuminance of $\approx 5 \times 10^4$ lux at a distance of $\frac{5}{8}$ in. (≈ 1.6 cm).

The LEDs are driven according to a pulse-width-modulation control scheme that makes it safe to drive the LEDs beyond their rated steady-state currents in order to generate additional light during short periods. The drive current and the pulse-width modulation for each LED panel can be controlled independently of those of the other 15

panels. The maximum allowable duration of each pulse of drive current is a function of the amount of overdrive, the total time to be spent in overdrive operation, and the limitations of the LEDs. The system is configured to limit the overdrive according to values specific to each type of LED in the array. These values are coded into firmware to prevent inadvertent damage to the LED panels.

This work was done by Dwayne Kiefer, Elizabeth Gray, and Robert Skupinski of QSS Group, Inc. and Arthur Stachowicz and William Birchenough of Zin Technologies, Inc. for Glenn Research Center. Further information is contained in a TSP (see page 1).

Inquiries concerning rights for the commercial use of this invention should be addressed to NASA Glenn Research Center, Innovative Partnerships Office, Attn: Steve Fedor, Mail Stop 4-8, 21000 Brookpark Road, Cleveland, Ohio 44135. Refer to LEW-17894-1.



Generic Environment for Simulating Launch Operations

GEM-FLO (A Generic Simulation Environment for Modeling Future Launch Operations) is a computer program that facilitates creation of discrete-event simulation models of ground processes in which reusable or expendable launch vehicles (RLVs) are prepared for flight. GEM-FLO includes a component, developed in Visual Basic, that generates a graphical user interface (GUI) and a component, developed in the Arena simulation language, that creates a generic discrete-event simulation model. Through the GUI, GEM-FLO elicits RLV design information from the user. The design information can include information on flight hardware elements, resources, and ground processes. GEM-FLO translates the user's responses into mathematical variables and expressions that populate the generic simulation model. The variables and expressions can represent processing times, resource capacities, status variables, and other process parameters needed to configure a simulation model that reflects the ground processing flow and requirements of a specific RLV. Upon execution of the model, GEM-FLO puts out data on many measures of performance, including the flight rate, turnaround time, and utilization of resources. This information can serve as the basis for determining whether design goals can be met, and for comparing characteristics of competing RLV designs.

This program was written by Martin Steele of Kennedy Space Center and Mansoor Mollaghasemi and Ghaith Rabadi of Productivity Apex, Inc. For further information, contact Mansoor Mollaghasemi at info@productivityapex.com. KSC-12488

Modular Aero-Propulsion System Simulation

The Modular Aero-Propulsion System Simulation (MAPSS) is a graphical simulation environment designed for the development of advanced control algorithms and rapid testing of these algorithms on a generic computational model of a turbofan engine and its con-

trol system. MAPSS is a nonlinear, non-real-time simulation comprising a Component Level Model (CLM) module and a Controller-and-Actuator Dynamics (CAD) module. The CLM module simulates the dynamics of engine components at a sampling rate of 2,500 Hz. The controller submodule of the CAD module simulates a digital controller, which has a typical update rate of 50 Hz. The sampling rate for the actuators in the CAD module is the same as that of the CLM. MAPSS provides a graphical user interface that affords easy access to engine-operation, engine-health, and control parameters; is used to enter such input model parameters as power lever angle (PLA), Mach number, and altitude; and can be used to change controller and engine parameters. Output variables are selectable by the user. Output data as well as any changes to constants and other parameters can be saved and reloaded into the GUI later.

This program was written by Khary I. Parker and Ten-Huei Guo of Glenn Research Center. Further information is contained in a TSP (see page 1).

Inquiries concerning rights for the commercial use of this invention should be addressed to NASA Glenn Research Center, Innovative Partnerships Office, Attn: Steve Fedor, Mail Stop 4-8, 21000 Brookpark Road, Cleveland, Ohio 44135. Refer to LEW-17674-1.

X-Windows Socket Widget Class

The X-Windows Socket Widget Class ("Class" is used here in the object-oriented-programming sense of the word) was devised to simplify the task of implementing network connections for graphical-user-interface (GUI) computer programs. UNIX Transmission Control Protocol/Internet Protocol (TCP/IP) socket programming libraries require many method calls to configure, operate, and destroy sockets. Most XWindows GUI programs use widget sets or toolkits to facilitate management of complex objects. The widget standards facilitate construction of toolkits and application programs. The X-Windows Socket Widget Class encapsulates UNIX TCP/IP socket-management tasks within the framework of an X Windows widget. Using the widget framework, X Windows GUI programs

can treat one or more network socket instances in the same manner as that of other graphical widgets, making it easier to program sockets. Wrapping ISP socket programming libraries inside a widget framework enables a programmer to treat a network interface as though it were a GUI.

This program was written by Matthew R. Barry of United Space Alliance for Johnson Space Center. For further information, contact the Johnson Innovative Partnerships Office at (281) 483-3809. MSC-23581

Infrastructure for Rapid Development of Java GUI Programs

The Java Application Shell (JAS) is a software framework that accelerates the development of Java graphical-user-interface (GUI) application programs by enabling the reuse of common, proven GUI elements, as distinguished from writing custom code for GUI elements. JAS is a software infrastructure upon which Java interactive application programs and graphical user interfaces (GUIs) for those programs can be built as sets of plug-ins. JAS provides an application-programming interface that is extensible by application-specific plugins that describe and encapsulate both specifications of a GUI and application-specific functionality tied to the specified GUI elements. The desired GUI elements are specified in Extensible Markup Language (XML) descriptions instead of in compiled code. JAS reads and interprets these descriptions, then creates and configures a corresponding GUI from a standard set of generic, reusable GUI elements. These elements are then attached (again, according to the XML descriptions) to application-specific compiled code and scripts. An application program constructed by use of JAS as its core can be extended by writing new plug-ins and replacing existing plug-ins. Thus, JAS solves many problems that Java programmers generally solve anew for each project, thereby reducing development and testing time.

This software was written by Jeremy Jones and Carl F. Hostetter of Goddard Space Flight Center and Philip Miller and Philip Wheeler of CommerceOne. Further information is contained in a TSP (see page 1). GSC-14769-1

Processing Raman Spectra of High-Pressure Hydrogen Flames

The Raman Code automates the analysis of laser-Raman-spectroscopy data for diagnosis of combustion at high pressure. On the basis of the theory of molecular spectroscopy, the software calculates the rovibrational and pure rotational Raman spectra of H₂, O₂, N₂, and H₂O in hydrogen/air flames at given temperatures and pressures. Given a set of Raman spectral data from measurements on a given flame and results from the aforementioned calculations, the software calculates the thermodynamic temperature and number densities of the aforementioned species. The software accounts for collisional spectral-line-broadening effects at pressures up to 60 bar (6 MPa). The line-broadening effects increase with pressure and thereby complicate the analysis. The software also corrects for spectral interference ("cross-talk") among the various chemical species. In the absence of such correction, the cross-talk is a significant source of error in temperatures and number densities. This is the first known comprehensive computer code that, when used in conjunction with a spectral calibration database, can process Raman-scattering spectral data from high-pressure hydrogen/air flames to obtain temperatures accurate to within ±10 K and chemical-species number densities accurate to within ±2 percent.

This work was done by Quang-Viet Nguyen of Glenn Research Center and Jun Kojima of the National Research Council. Further information is contained in a TSP (see page 1).

Inquiries concerning rights for the commercial use of this invention should be addressed to NASA Glenn Research Center, Innovative Partnerships Office, Attn: Steve Fedor, Mail Stop 4-8, 21000 Brookpark Road, Cleveland, Ohio 44135. Refer to LEW-17769-1.

X-Windows Information Sharing Protocol Widget Class

The X-Windows Information Sharing Protocol (ISP) Widget Class ("Class" is used here in the object-oriented-programming sense of the word) was devised to simplify the task of implementing ISP graphical-user-interface (GUI) computer programs. ISP programming tasks require many method calls to identify, query, and in-

terpret the connections and messages exchanged between a client and an ISP server. Most X-Windows GUI programs use widget sets or toolkits to facilitate management of complex objects. The widget standards facilitate construction of toolkits and application programs. The X-Windows Information Sharing Protocol (ISP) Widget Class encapsulates the client side of the ISP programming libraries within the framework of an X-Windows widget. Using the widget framework, X-Windows GUI programs can interact with ISP services in an abstract way and in the same manner as that of other graphical widgets, making it easier to write ISP GUI client programs. Wrapping ISP client services inside a widget framework enables a programmer to treat an ISP server interface as though it were a GUI. Moreover, an alternate subclass could implement another communication protocol in the same sort of widget.

This program was written by Matthew R. Barry of United Space Alliance for Johnson Space Center. For further information, contact the Johnson Innovative Partnerships Office at (281) 483-3809. MSC-23583

Simulating Humans as Integral Parts of Spacecraft Missions

The Collaborative-Virtual Environment Simulation Tool (C-VEST) software was developed for use in a NASA project entitled "3-D Interactive Digital Virtual Human." The project is oriented toward the use of a comprehensive suite of advanced software tools in computational simulations for the purposes of human-centered design of spacecraft missions and of the spacecraft, space suits, and other equipment to be used on the missions. The C-VEST software affords an unprecedented suite of capabilities for three-dimensional virtual-environment simulations with plug-in interfaces for physiological data, haptic interfaces, plug-and-play software, real-time control, and/or playback control. Mathematical models of the mechanics of the human body and of the aforementioned equipment are implemented in software and integrated to simulate forces exerted on and by astronauts as they work. The computational results can then support the iterative processes of design, building, and testing in applied systems engineering and integration. The results of the simula-

tions provide guidance for devising measures to counteract effects of microgravity on the human body and for the rapid development of virtual (that is, simulated) prototypes of advanced space suits, cockpits, and robots to enhance the productivity, comfort, and safety of astronauts. The unique ability to implement human-in-the-loop immersion also makes the C-VEST software potentially valuable for use in commercial and academic settings beyond the original space-mission setting.

This program was written by Anthony C. Bruins of Johnson Space Center; Robert Rice of Dynoverse Corp.; Lac Nguyen, Heidi Nguyen, and Tim Saito of HPN Software Consultant, Inc.; and Elaine Russell of the Institute of Somatic Sciences. For further information, contact the Johnson Innovative Partnerships Office at (281) 483-3809. MSC-23454

Analyzing Power Supply and Demand on the ISS

Station Power and Energy Evaluation Determiner (SPEED) is a Java application program for analyzing the supply and demand aspects of the electrical power system of the International Space Station (ISS). SPEED can be executed on any computer that supports version 1.4 or a subsequent version of the Java Runtime Environment. SPEED includes an analysis module, denoted the Simplified Battery Solar Array Model, which is a simplified engineering model of the ISS primary power system. This simplified model makes it possible to perform analyses quickly. SPEED also includes a user-friendly graphical-interface module, an input file system, a parameter-configuration module, an analysis-configuration-management subsystem, and an output subsystem. SPEED responds to input information on trajectory, shadowing, attitude, and pointing in either a state-of-charge mode or a power-availability mode. In the state-of-charge mode, SPEED calculates battery state-of-charge profiles, given a time-varying power-load profile. In the power-availability mode, SPEED determines the time-varying total available solar array and/or battery power output, given a minimum allowable battery state of charge.

This work was done by Justin Thomas, Tho Pham, Raymond Halyard, and Steve Conwell of United Space Alliance for Johnson Space Center. For further information, contact the Johnson Innovative Partnerships Office at (281) 483-3809. MSC-23621



Polyimides From a-BPDA and Aromatic Diamines

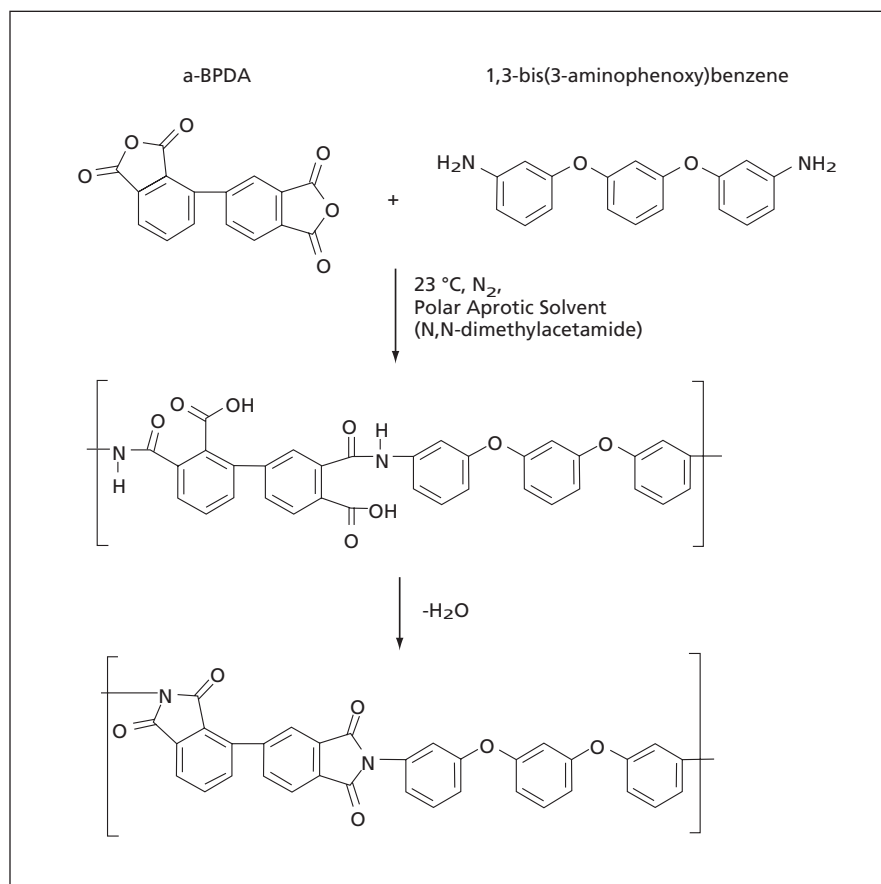
These polyimides have low color and high mechanical properties.

Langley Research Center, Hampton, Virginia

Polymers having low color and a favorable combination of other properties, including high glass-transition temperature (T_g) and high mechanical properties (strength, tensile modulus, and toughness) will find use in a variety of terrestrial and space applications. Some of the space applications will be in thin films used as membranes on antennas, solar concentrators, coatings on second-surface mirrors, solar sails, sunshades, thermal and optical coatings, and multi-layer thermal insulation blankets. Depending upon the application, the film will be required to exhibit a unique combination of such properties as resistance to degradation by ultraviolet light, visible light, and electrons; low color and/or low solar absorptivity; resistance to tearing and/or wrinkling during packaging and deployment; and high mechanical properties (e.g. high strength, stiffness, and toughness). Recently developed polyimides having several of these desired properties are described below.

These polyimides were prepared by reacting a unique aromatic dianhydride — 2,3,3',4'-biphenyltetracarboxylic dianhydride (a-BPDA) — in polar aprotic solvents with aromatic diamines. The selection of the aromatic diamines enabled the tailoring of the polyimides to obtain low color plus combinations of other properties desired for specific applications.

In the example of the figure, a-BPDA was reacted with 1,3-bis(3-aminophenoxy)benzene in N,N-dimethylacetamide, at a solids content of 20 weight percent, to obtain a polyamide acid having an inherent viscosity of 0.73 dL/g. A thin film cast from the polyamide acid on plate glass was stage-dried for 1 hour at a temperature of 250 °C in air. The 0.066-mm thick film was nearly colorless and exhibited a transparency of 86 percent at a wavelength of 500 nm. The T_g of the film was found to be 207 °C. At a temperature of 23 °C, the film exhibited the following tensile properties: strength of 16 kpsi (\approx 110 MPa), modulus of 476 kpsi (\approx 3.28 GPa), and elongation of 6 percent. The film acquired a pale yellow color when it was further cured for 1 hour at 350 °C in air. The T_g increased to 209 °C and the



A Low-Color Polyimide Was Synthesized from a-BPDA and 1,3-bis(3-aminophenoxy)benzene.

tensile properties at 23 °C changed slightly to strength of 18 kpsi (\approx 124 MPa), modulus of 476 kpsi (\approx 3.28 GPa), and elongation of 5.7 percent.

Polyimides derived from a-BPDA exhibited less color, and, accordingly, lower solar absorptivity and thermal emissivity, than did polyimides in general and particularly the corresponding polyimides made from the symmetric dianhydride, 3,3',4,4'-biphenyltetracarboxylic dianhydride. The latter two properties are particularly important for use in outer space. Solar absorptivity pertains to the fraction of incoming solar energy that is absorbed by the film or, more precisely, a measure of light reflected by a second-surface mirror at wavelengths between 250 and 2,800 nm. The thermal emissivity is a measure of the ability of a film to radiate energy from its

surface or, more precisely, a measure of the infrared transmission of the film. The ratio between solar absorptivity and thermal emissivity is more important than are the individual values of solar absorptivity and thermal emissivity because this ratio is more directly indicative of the temperature that a film or surface will attain in a particular orbit. Polyimides derived from a-BPDA have highly irregular structures that contribute to lower melt viscosities, and higher T_g s, than those of polyimides derived from the symmetric dianhydride.

This work was done by Paul M. Hergenrother, Joseph G. Smith, Jr., and John W. Connell of Langley Research Center and Kent A. Watson of the National Institute of Aerospace. For further information, contact the Intellectual Property Team at (757) 864-3521. LAR-16430-1

Making Plant-Support Structures From Waste Plant Fiber

John F. Kennedy Space Center, Florida

Environmentally benign, biodegradable structures for supporting growing plants can be made in a process based on recycling of such waste plant fiber materials as wheat straw or of such derivative materials as paper and cardboard. Examples of structures that can be made in this way include plant plugs, pots, planter-lining mats, plant fences, and root and shoot barriers. No chemical binders are used in the process. First, the plant material is chopped into smaller particles. The particles are leached with water or steam to remove material that can inhibit plant growth, yielding a fibrous slurry. If the desired structures are

plugs or sheets, then the slurry is formed into the desired shapes in a pulp molding subprocess. If the desired structures are root and shoot barriers, pots, or fences, then the slurry is compression-molded to the desired shapes in a heated press. The processed materials in these structures have properties similar to those of commercial pressboard, but unlike pressboard, these materials contain no additives. These structures have been found to withstand one growth cycle, even when wet.

This work was done by Robert C. Morrow, Matthew J. Mischnick, Amanda Pertzborn, and Chad Ehle of Orbital Technologies Corp.

*and John Hunt of the United States Department of Agriculture Forest Products Laboratory for **Kennedy Space Center**.*

In accordance with Public Law 96-517, the contractor has elected to retain title to this invention. Inquiries concerning rights for its commercial use should be addressed to:

Robert Morrow

Orbital Technologies Corp.

1212 Fowier Drive, Madison, WI 53717

Phone: (608) 827-5000

E-mail: morrowr@orbitec.com.

Refer to KSC-12585, volume and number of this NASA Tech Briefs issue, and the page number.



Large Deployable Reflectarray Antenna

NASA's Jet Propulsion Laboratory, Pasadena, California

A report discusses a 7-meter-diameter reflectarray antenna that has been conceived in a continuing effort to develop large reflectarray antennas to be deployed in outer space. Major underlying concepts were reported in three prior *NASA Tech Briefs* articles: "Inflatable Reflectarray Antennas" (NPO-20433), Vol. 23, No. 10 (October 1999), page 50; "Tape-Spring Reinforcements for Inflatable Structural Tubes" (NPO-20615), Vol. 24, No. 7 (July 2000), page 58; and "Self-Inflatable/Self-Rigidizable Reflectarray Antenna" (NPO-

30662), Vol. 28, No. 1 (January 2004), page 61. Like previous antennas in the series, the antenna now proposed would include a reflectarray membrane stretched flat on a frame of multiple inflatable booms. The membrane and booms would be rolled up and folded for compact stowage during transport. Deployment in outer space would be effected by inflating the booms to unroll and then to unfold the membrane, thereby stretching the membrane out flat to its full size. The membrane would achieve the flatness for

a Ka-band application. The report gives considerable emphasis to designing the booms to rigidify themselves upon deployment: for this purpose, the booms could be made as spring-tape-reinforced aluminum laminate tubes like those described in two of the cited prior articles.

This work was done by Houfei Fang, John Huang, and Michael Lou of Caltech for NASA's Jet Propulsion Laboratory. Further information is contained in a TSP (see page 1). NPO-41083

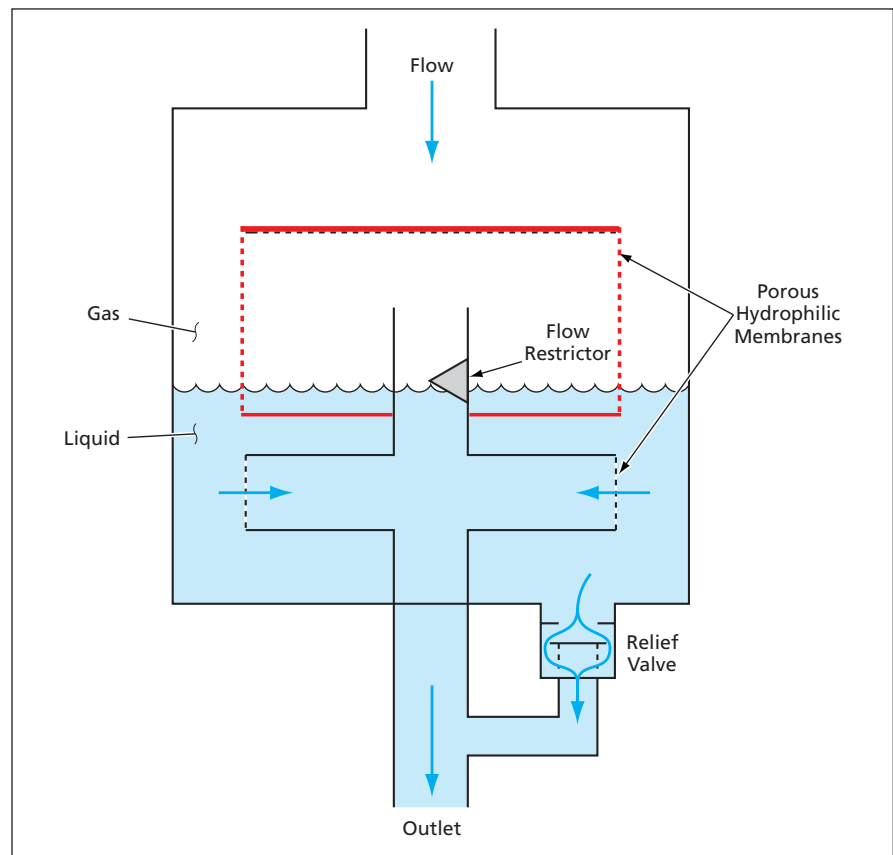
Periodically Discharging, Gas-Coalescing Filter

In effect, small bubbles would be made to coalesce into very large ones.

Marshall Space Flight Center, Alabama

A proposed device would remove bubbles of gas from a stream of liquid (typically water), accumulate the gas, and periodically release the gas, in bulk, back into the stream. The device is intended for use in a flow system (1) in which there is a requirement to supply bubble-free water to a downstream subsystem and (2) that includes a sensor and valves, just upstream of the subsystem, for sensing bubbles and diverting the flow from the subsystem until the water stream is again free of bubbles. By coalescing the gas bubbles and then periodically releasing the accumulated gas, the proposed device would not contribute to net removal of gas from the liquid stream; nevertheless, it would afford an advantage by reducing the frequency with which the diverter valves would have to be activated.

The device (see figure) would include an upper and a lower porous membrane made of a hydrophilic material. Both membranes would cover openings in a tube leading to an outlet. These membranes would allow water, but not gas bubbles, to pass through to the interior of the tube. Inside the tube, between the two membranes, there would be a flow restrictor that would play a role described below. Below both membranes there would be a relief valve.



Gas From Trapped Bubbles Would Accumulate in the head space in this vessel until the water level fell below the lower hydrophilic membrane. Then the relief valve would open, releasing the gas and water to the outlet.

Water, possibly containing bubbles, would enter from the top and would pass through either the lower membrane or both membranes, depending how much gas had been accumulated thus far. When the volume of accumulated gas was sufficient to push the top surface of the liquid below the lower porous membrane, water could no longer flow through either membrane

toward the outlet. This blockage would cause an increase in back pressure that would cause the relief valve to open. The opening of the relief valve would allow both the water and the bulk-accumulated gas to pass through to the outlet. Once the gas had been pushed out, water would once again flow through both membranes at a much lower pressure drop. The flow restrictor would

maintain enough pressure drop to keep the relief valve open until gas had been cleared from both hydrophilic membranes.

*This work was done by Donald Layne Carter and Donald W. Holder of **Marshall Space Flight Center** and Edward W. O'Connor of Hamilton Sundstrand. Further information is contained in a TSP (see page 1).
MFS-31930*



Ion Milling On Steps for Fabrication of Nanowires

This process could readily be scaled up for mass production.

NASA's Jet Propulsion Laboratory, Pasadena, California

Arrays of nanowires having controlled dimensions can now be fabricated on substrates, optionally as integral parts of multilayer structures, by means of a cost-effective, high-yield process based on ion milling on steps. Nanowires made, variously, of semiconductors or metals are needed as compo-

nents of sensors and high-density electronic circuits.

Unlike prior processes used to fabricate nanowires, the present process does not involve electron-beam lithography, manipulation of nanoscopic objects by use of an atomic-force microscope, or any other technique that is inherently

unsuitable for scaling up to mass production. In comparison with the prior processes, this process is rapid and simple. Wires having widths as small as a few tens of nanometers and lengths as long as millimeters have been fabricated by use of this process.

The figure depicts a workpiece at different stages of the process. A silicon dioxide substrate is coated with a photoresist or poly(methyl methacrylate) [PMMA] to a thickness of as much as 500 nm. The photoresist or PMMA is patterned to form edges where wires are to be formed. A metal — either Pt or Ti — is deposited, by sputtering, to a thickness of as much as 200 nm. By ion milling at normal incidence, the thickness of the metal deposit is reduced until the only metal that remains is in the form of wall-like nanowires along the edges of the photoresist or PMMA. Finally, an oxygen plasma is used to remove the photoresist or PMMA, leaving only the nanowires on the substrate.

This work was done by Minhee Yun, Richard Vasquez, and Choonsup Lee of Caltech for NASA's Jet Propulsion Laboratory. Further information is contained in a TSP (see page 1).

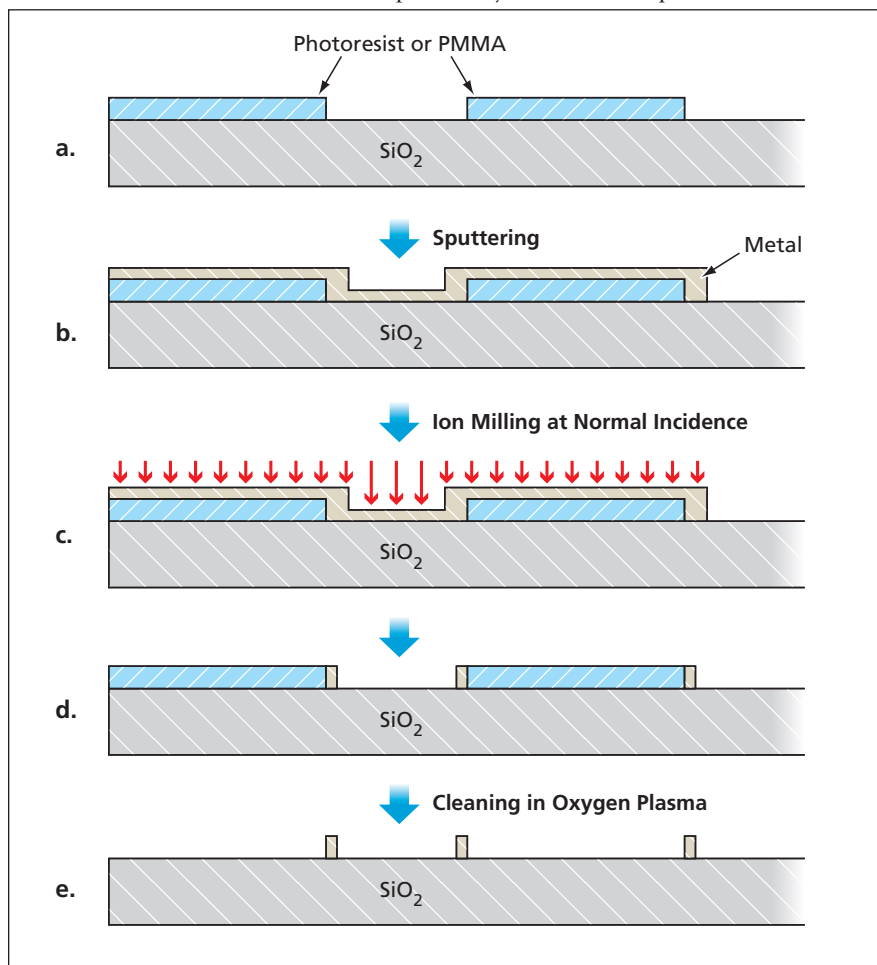
In accordance with Public Law 96-517, the contractor has elected to retain title to this invention. Inquiries concerning rights for its commercial use should be addressed to:

*Innovative Technology Assets Management
JPL*

*Mail Stop 202-233
4800 Oak Grove Drive
Pasadena, CA 91109-8099
(818) 354-2240*

E-mail: iaoffice@jpl.nasa.gov

Refer to NPO-40933, volume and number of this NASA Tech Briefs issue, and the page number.



Wall-Like Nanowires are formed at the edges of the photoresist or PMMA when the thickness of the metal is reduced by ion milling at normal incidence.



Neuro-Prosthetic Implants With Adjustable Electrode Arrays

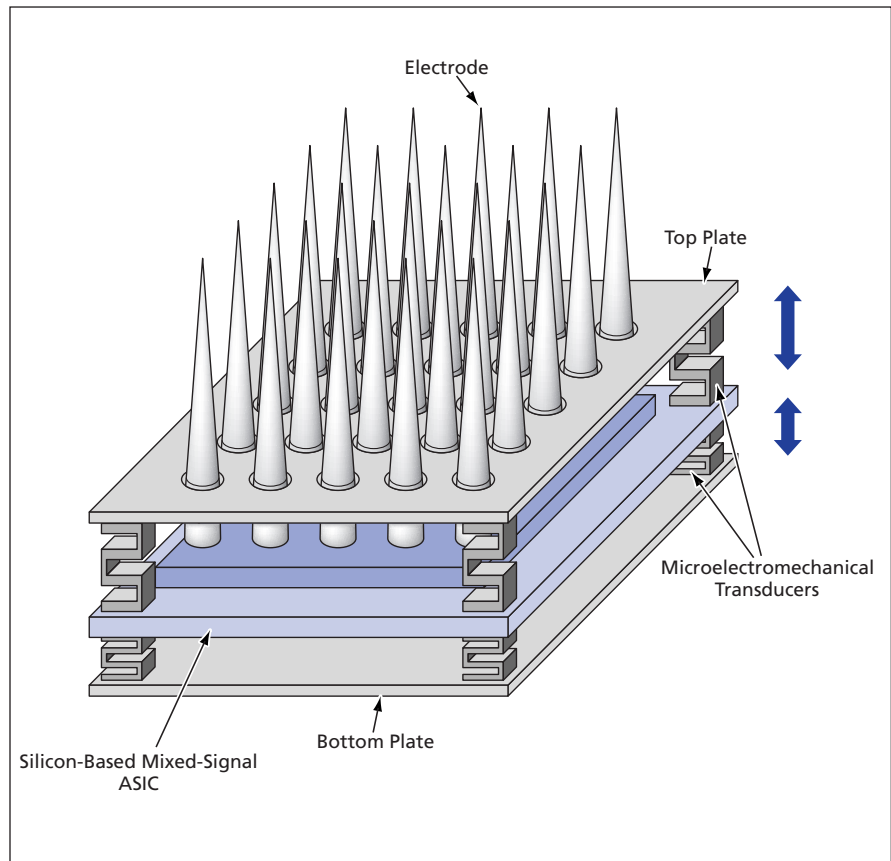
Depths of penetration of electrodes would be adjusted to maximize received signals.

NASA's Jet Propulsion Laboratory, Pasadena, California

Brushlike arrays of electrodes packaged with application-specific integrated circuits (ASICs) are undergoing development for use as electronic implants — especially as neuro-prosthetic devices that might be implanted in brains to detect weak electrical signals generated by neurons. These implants partly resemble the ones reported in “Integrated Electrode Arrays for Neuro-Prosthetic Implants” (NPO-21198), *NASA Tech Briefs*, Vol. 27, No. 2 (February 2003), page 48. The basic idea underlying both the present and previously reported implants is that the electrodes would pick up signals from neurons and the ASICs would amplify and otherwise preprocess the signals for monitoring by external equipment.

The figure presents a simplified and partly schematic view of an implant according to the present concept. Whereas the electrodes in an implant according to the previously reported concept would be microscopic wires, the electrodes according to the present concept are in the form of microscopic needles. An even more important difference would be that, unlike the previously reported concept, the present concept calls for the inclusion of microelectromechanical actuators for adjusting the depth of penetration of the electrodes into brain tissue.

The prototype implant now under construction includes an array of 100 electrodes and corresponding array of electrode contact pads formed on opposite faces of a plate fabricated by techniques that are established in the art of microelectromechanical systems (MEMS). A mixed-signal ASIC under construction at the time of reporting the information for this article will include 100 analog amplifier channels (one amplifier per electrode). On one face of the mixed-signal ASIC there will be a solder-bump/micro-pad array that will have the same pitch as that of the electrode array, and that will be used to make the electrical and mechanical connections between the electrode array and the ASIC. Once the electrode



The Thickness of the Implant Package and/or the length of protrusion of the electrodes would be adjusted by use of the microelectromechanical actuators.

array and the ASIC are soldered together, the remaining empty space between them will be filled with a biocompatible epoxy, the remaining exposed portions of the ASIC will be covered with micromachined plates for protection against corrosive bodily fluids, and then the ASIC and its covering micromachined plates will be coated with parylene.

The implant includes a top plate, into which through-holes of the same pitch as that of the electrodes have been micromachined. The plate is mounted so that the electrodes protrude through the holes. The implant also includes a bottom plate without through-holes. The depth of penetration of the electrodes into brain tissue (more precisely, the thickness of, and

the length of protrusion of the electrodes from, the implant package) would be controlled by use of microelectromechanical actuators that would move the top and bottom plates toward or away from the MEMS electrode-supporting plate.

The microelectromechanical actuators would be controlled by electrical signals from the ASIC. According to one concept under consideration at press time, the actuators could be microfabricated electrochemical cells containing solid electrolytes that expand by large amounts (increase in thickness of the order of 50 percent) when charged to potentials of the order of 3 V. The control signals for the transducers could originate in external equipment or could be gener-

ated by an on-chip servocontrol subsystem that would strive to adjust the depth of penetration to maximize the strength of signals picked up by the electrodes. The ASIC will include a section for induction and/or radio reception of power and control signals from, and for transmission of electrode readout signals to, external equipment. A simple wire dipole antenna or a printed spiral coil on a flexible substrate could be used to couple

the signals between the implant and external equipment, without need for wire connections.

This work was done by Jay Whitacre, Linda Y. Del Castillo, Mohammad Mojarradi, Travis Johnson, William West, and Richard Andersen of Caltech for NASA's Jet Propulsion Laboratory. Further information is contained in a TSP (see page 1).

In accordance with Public Law 96-517, the contractor has elected to retain title to this

invention. Inquiries concerning rights for its commercial use should be addressed to:

*Innovative Technology Assets Management
JPL*

*Mail Stop 202-233
4800 Oak Grove Drive
Pasadena, CA 91109-8099
(818) 354-2240*

E-mail: iaoffice@jpl.nasa.gov

Refer to NPO-30516, volume and number of this NASA Tech Briefs issue, and the page number.

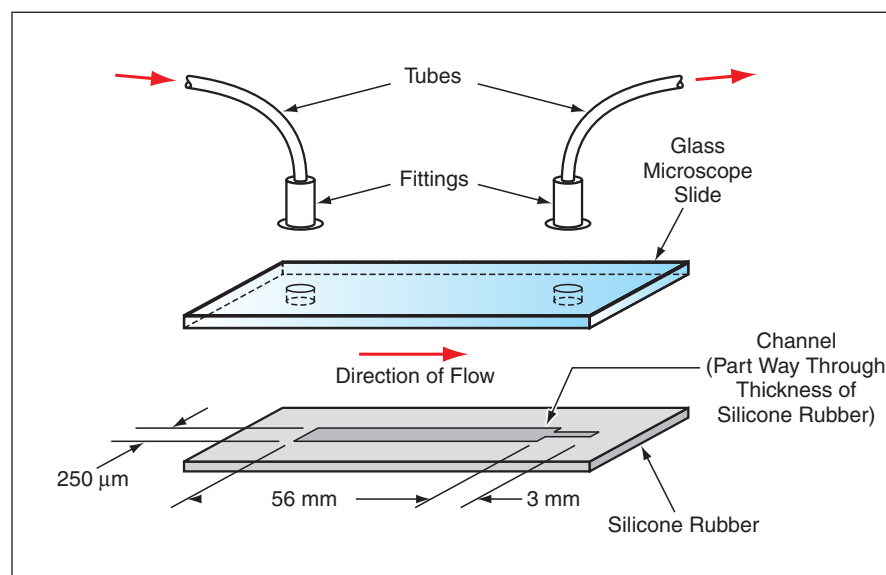
Microfluidic Devices for Studying Biomolecular Interactions

These devices can be fabricated rapidly and inexpensively.

Marshall Space Flight Center, Alabama

Microfluidic devices for monitoring biomolecular interactions have been invented. These devices are basically highly miniaturized liquid-chromatography columns. They are intended to be prototypes of miniature analytical devices of the "laboratory on a chip" type that could be fabricated rapidly and inexpensively and that, because of their small sizes, would yield analytical results from very small amounts of expensive analytes (typically, proteins). Other advantages to be gained by this scaling down of liquid-chromatography columns may include increases in resolution and speed, decreases in the consumption of reagents, and the possibility of performing multiple simultaneous and highly integrated analyses by use of multiple devices of this type, each possibly containing multiple parallel analytical microchannels.

The principle of operation is the same as that of a macroscopic liquid-chromatography column: The column is a channel packed with particles, upon which are immobilized molecules of the protein of interest (or one of the proteins of interest if there are more than one). Starting at a known time, a solution or suspension containing molecules of the protein or other substance of interest is pumped into the channel at its inlet. The liquid emerging from the outlet of the channel is monitored to detect the molecules of the dissolved or suspended substance(s). The time that it takes these molecules to flow from the inlet to the outlet is a measure of the degree of interaction between the immobilized and the dissolved or suspended molecules. Depending on the precise natures of the molecules, this measure can be used for diverse purposes: exam-



A Basic Microfluidic Device according to the invention includes a sheet of silicone rubber containing a molded channel that is exposed at its upper surface. The sheet is sealed to a glass microscope slide, thereby enclosing the channel.

ples include screening for solution conditions that favor crystallization of proteins, screening for interactions between drugs and proteins, and determining the functions of biomolecules.

The figure presents a schematic exploded view of a basic microfluidic device according to the invention. The device includes a sheet of polydimethylsiloxane (silicone rubber) that contains the channel and that is sealed to a glass microscope slide. In order to make this sheet, one first makes a mold that comprises a flat surface from which protrudes a ridge having the dimensions of the channel. The mold can be fabricated photolithographically on an oxidized silicon substrate. The silicone-rubber sheet is formed by casting the

mixture of silicone-rubber ingredients on the mold.

Prior to assembly, a diamond-tipped drill is used to make holes in the microscope slide at the locations assigned to the inlet and outlet ends of the channel. After cleaning and oxidizing in an air plasma cleaner, the silicone-rubber sheet and the microscope slide are pressed together, taking care to align the holes with the ends of the channels. No adhesive is needed; an irreversible seal is formed spontaneously between the glass and the silicone rubber.

Fittings for tubes to carry the liquid are attached to the edges of the holes in the microscope slide. Particles coated with the substance to be immobilized in the column are suspended in a slurry,

which is then flushed along the channel. The channel is narrowed at its outlet end by an amount determined by the size of the particles, such that particles that arrive at the outlet become stuck there, preventing themselves and any others from flowing out of the channel (this phenomenon is known in the art as the keystone effect). As a result, the continued flushing with the slurry causes

the channel to become packed with the particles.

This work was done by Wilbur W. Wilson and Carlos D. Garcia of Mississippi State University and Charles S. Henry of Colorado State University for Marshall Space Flight Center.

In accordance with Public Law 96-517, the contractor has elected to retain title to this invention. Inquiries concerning rights for its

commercial use should be addressed to:

*Mississippi State University
Office of Intellectual Property and Technology Licensing
P.O. Box 5282
Mississippi State, MS 39762
Phone: (662) 325-9263*

Refer to MFS-31978-1, volume and number of this NASA Tech Briefs issue, and the page number.

Studying Functions of All Yeast Genes Simultaneously

This method could accelerate research on treatment of some diseases.

Ames Research Center, Moffett Field, California

A method of studying the functions of all the genes of a given species of microorganism simultaneously has been developed in experiments on *Saccharomyces cerevisiae* (commonly known as baker's or brewer's yeast). It is already known that many yeast genes perform functions similar to those of corresponding human genes; therefore, by facilitating understanding of yeast genes, the method may ultimately also contribute to the knowledge needed to treat some diseases in humans.

Because of the complexity of the method and the highly specialized nature of the underlying knowledge, it is possible to give only a brief and sketchy summary here. The method involves the use of unique synthetic deoxyribonucleic

acid (DNA) sequences that are denoted as DNA bar codes because of their utility as molecular labels. The method also involves the disruption of gene functions through deletion of genes. *Saccharomyces cerevisiae* is a particularly powerful experimental system in that multiple deletion strains easily can be pooled for parallel growth assays. Individual deletion strains recently have been created for 5,918 open reading frames, representing nearly all of the estimated 6,000 genetic loci of *Saccharomyces cerevisiae*.

Tagging of each deletion strain with one or two unique 20-nucleotide sequences enables identification of genes affected by specific growth conditions, without prior knowledge of gene functions. Hybridization of bar-code DNA to

oligonucleotide arrays can be used to measure the growth rate of each strain over several cell-division generations. The growth rate thus measured serves as an index of the fitness of the strain.

This work was done by Viktor Stolz of Ames Research Center; Robert G. Eason, Nader Pourmand, Zelek S. Herman, and Ronald W. Davis of Stanford Genome Technology Center; Waraporn Tongprasit of ELORET Corp.; and Kevin Anthony and Olufisayo Jejelowo of Texas Southern University. Further information is contained in a TSP (see page 1).

Inquiries concerning rights for the commercial use of this invention should be addressed to the Innovative Partnerships Office, Ames Research Center, (650) 604-2954. Refer to ARC-15345-1.



Polarization Phase-Compensating Coats for Metallic Mirrors

NASA's Jet Propulsion Laboratory, Pasadena, California

A method of compensating for or minimizing phase differences between orthogonal polarizations of light reflected from metallic mirrors at oblique incidence, as, for example, from weakly curved mirrors, is undergoing development. The method is intended to satisfy a need to maintain precise polarization phase relationships or minimum polarization differences needed for proper operation of telescopes and other scientific instruments that include single or multiple mirrors. The basic idea of the method is to optimally coat mirrors with thin engineered layers of materials that introduce phase differences that, as nearly precisely as possible, are opposite of

the undesired phase differences arising in reflection with non-optimum coatings. Depending on the specific optical system, the method could involve any or all of the following elements:

- Optimization of a single coat on all the mirrors in the system.
- Optimization of a unique coat for each mirror such that the polarization phase effects of the coat on one mirror compensate, to an acceptably high degree over an acceptably wide wavelength range, for those of the coat on another mirror.
- Tapering the coat on each mirror. Optimization could involve the choice

of a single dielectric coating material and its thickness, or design of a more-complex coat consisting of multiple layers of different dielectric materials and possibly some metallic materials. Such designs and coatings are particularly significant and needed for obtaining very high quality of wavefront required in high-contrast imaging instruments such as the NASA Terrestrial Planet Finder Coronagraph.

This work was done by Kunjithapatham Balasubramanian of Caltech for NASA's Jet Propulsion Laboratory. Further information is contained in a TSP (see page 1). NPO-41396

Tunable-Bandwidth Filter System

Pass bands can be tuned rapidly across the visible and near infrared spectrum.

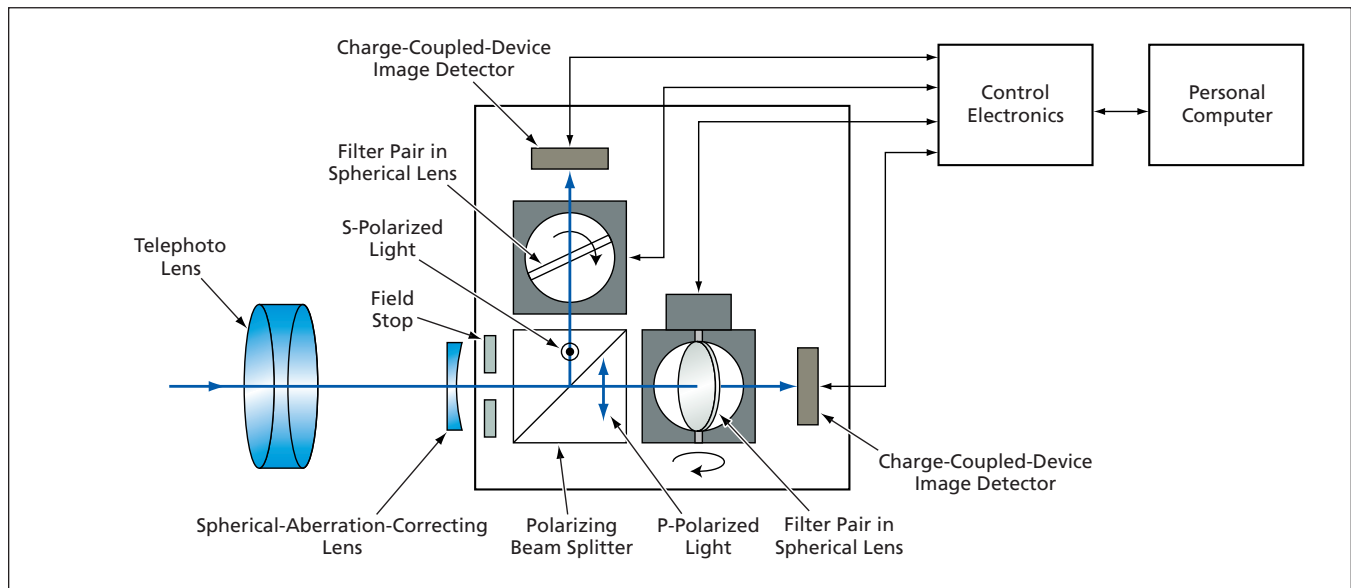
Stennis Space Center, Mississippi

A tunable-bandwidth filter system (TBFS), now undergoing development, is intended to be part of a remote-sensing multispectral imaging system that will operate in the visible and near infrared spectral region (wavelengths from 400 to 900 nm). Attributes of the TBFS include

rapid tunability of the pass band over a wide wavelength range and high transmission efficiency. The TBFS is based on a unique integration of two pairs of broadband Raman reflection holographic filters with two rotating spherical lenses. In experiments, a prototype of the

TBFS was shown to be capable of spectral sampling of images in the visible range over a 200-nm spectral range with a spectral resolution of ≈ 30 nm.

The figure depicts the optical layout of a prototype of the TBFS as part of a laboratory multispectral imaging sys-



A Laboratory Prototype of the TBFS contains two rotating spherical lenses containing broadband Raman reflection holographic filters. The pass band of each filter varies with the angle of incidence. Hence, the rotations are coordinated to obtain coordinated variations of the pass bands with time.

tem for the spectral sampling of color test images in two orthogonal polarizations. Each pair of broadband Raman reflection holographic filters is mounted at an equatorial plane between two halves of a spherical lens. The two filters in each pair are characterized by steep spectral slopes (equivalently, narrow spectral edges), no ripple or side lobes in their pass bands, and a few nanometers of non-overlapping wavelength range between their pass bands. Each spherical lens and thus the filter pair within it is rotated in order to rapidly tune its pass band. The rotations of the lenses are effected by electronically controlled, programmable,

high-precision rotation stages. The rotations are coordinated by electronic circuits operating under overall supervision of a personal computer in order to obtain the desired variation of the overall pass bands with time.

Embedding the filters inside the spherical lenses increases the range of the hologram incidence angles, making it possible to continuously tune the pass and stop bands of the filters over a wider wavelength range. In addition, each spherical lens also serves as part of the imaging optics: The telephoto lens focuses incoming light to a field stop that is also a focal point of each spherical lens. A correcting lens in front of the

field stop compensates for the spherical aberration of the spherical lenses. The front surface of each spherical lens collimates the light coming from the field stop. After the collimated light passes through the filter in the spherical lens, the rear surface of the lens focuses the light onto a charge-coupled-device image detector.

This work was done by Tin Aye, Kevin Yu, Fedor Dimov, and Gajendra Savant of Physical Optics Corp. for Stennis Space Center.

Inquiries concerning rights for the commercial use of this invention should be addressed to the Intellectual Property Manager, Stennis Space Center, (228) 688-1929. Refer to SSC-00210-1.



Methodology for Designing Fault-Protection Software

A document describes a methodology for designing fault-protection (FP) software for autonomous spacecraft. The methodology embodies and extends established engineering practices in the technical discipline of Fault Detection, Diagnosis, Mitigation, and Recovery; and has been successfully implemented in the Deep Impact Spacecraft, a NASA Discovery mission. Based on established concepts of Fault Monitors and Responses, this FP methodology extends the notion of Opinion, Symptom, Alarm (aka Fault), and Response with numerous new notions, sub-notions, software constructs, and logic and timing gates. For example, Monitor generates a RawOpinion, which graduates into Opinion, categorized into no-opinion, acceptable, or unacceptable opinion. RaiseSymptom, ForceSymptom, and ClearSymptom govern the establishment and then mapping to an Alarm (aka Fault). Local Response is distinguished from FP System Response. A 1-to- n and n -to-1 mapping is established among Monitors, Symptoms, and Responses. Responses are categorized by device versus by function. Responses operate in tiers, where the early tiers attempt to resolve the Fault in a localized step-by-step fashion, relegating more system-level response to later tier(s). Recovery actions are gated by epoch recovery timing, enabling strategy, urgency, MaxRetry gate, hardware availability, hazardous versus ordinary fault, and

many other priority gates. This methodology is systematic, logical, and uses multiple linked tables, parameter files, and recovery command sequences. The credibility of the FP design is proven via a fault-tree analysis “top-down” approach, and a functional fault-mode-effects-and-analysis via “bottoms-up” approach. Via this process, the mitigation and recovery strategy(s) per Fault Containment Region scope (width versus depth) the FP architecture.

This work was done by Kevin Barltrop, Jeffrey Levison, and Edwin Kan of Caltech for NASA's Jet Propulsion Laboratory. Further information is contained in a TSP (see page 1).

The software used in this innovation is available for commercial licensing. Please contact Karina Edmonds of the California Institute of Technology at (818) 393-2827. Refer to NPO-41344.

Ground-Based Localization of Mars Rovers

The document discusses a procedure for localizing the Mars rovers in site frame, a locally defined reference frame on the Martian surface. MER onboard position within a site frame is estimated onboard and is based on wheel odometry. Odometry estimation of rover position is only reliable over relatively short distances assuming no wheel slip, sinkage, etc. As the rover traverses, its onboard estimate of position in the current site frame accumulates errors and will need to be corrected on occasions via relocalization on the ground (mission operations). The procedure pro-

vides a systematic process for ground operators to localize the rover. The method focuses on analysis of acquired images used to declare a site frame and images acquired post-drive. Target selection is performed using two main steps. In the first step, the user identifies features of interest from the images used to declare the current site. Each of the selected target's position in site frame is recorded. In the second step, post-traverse measurements of the selected features' positions are recorded again, this time in rover frame, using images acquired post-traverse. In the third step, we transform the post-traverse target's positions to local level frame. In the fourth step, we compute the delta differences in the pre- and post-traverse target's position. In the fifth step, we analyze the delta differences with techniques that compute their statistics to determine the rover's position in the site frame.

This work was done by Ashitey Trebi-Ollennu of Caltech for NASA's Jet Propulsion Laboratory.

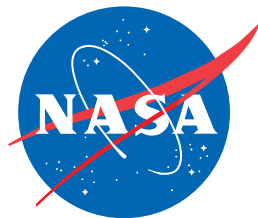
In accordance with Public Law 96-517, the contractor has elected to retain title to this invention. Inquiries concerning rights for its commercial use should be addressed to:

*Innovative Technology Assets Management
JPL*

*Mail Stop 202-233
4800 Oak Grove Drive
Pasadena, CA 91109-8099
(818) 354-2240*

E-mail: iaoffice@jpl.nasa.gov

Refer to NPO-41701, volume and number of this NASA Tech Briefs issue, and the page number.]



National Aeronautics and
Space Administration